Molecular Cell
Short Article

Quiescence-Induced LncRNAs Trigger H4K20 Trimethylation and Transcriptional Silencing

Holger Bierhoff,[1] Marcel Andre Dammert,[1] David Brocks,[1] Silvia Dambacher,[2] Gunnar Schotta,[2] and Ingrid Grummt[1,*]
[1]Division of Molecular Biology of the Cell II, German Cancer Research Center, DKFZ-ZMBH Alliance, 69120 Heidelberg, Germany
[2]Adolf Butenandt Institute and Center for Integrated Protein Science Munich, Ludwig-Maximilians-Universität, 80336 Munich, Germany
*Correspondence: i.grummt@dkfz.de
http://dx.doi.org/10.1016/j.molcel.2014.03.032

SUMMARY

A complex network of regulatory pathways links transcription to cell growth and proliferation. Here we show that cellular quiescence alters chromatin structure by promoting trimethylation of histone H4 at lysine 20 (H4K20me3). In contrast to pericentric or telomeric regions, recruitment of the H4K20 methyltransferase Suv4-20h2 to rRNA genes and IAP elements requires neither trimethylation of H3K9 nor interaction with HP1 proteins but depends on long noncoding RNAs (lncRNAs) that interact with Suv4-20h2. Growth factor deprivation and terminal differentiation lead to upregulation of these lncRNAs, increase in H4K20me3, and chromatin compaction. The results uncover a lncRNA-mediated mechanism that guides Suv4-20h2 to specific genomic loci to establish a more compact chromatin structure in growth-arrested cells.

INTRODUCTION

In the past few years, thousands of long noncoding RNAs (lncRNAs) have been identified, originating from intergenic or coding regions in sense or antisense orientation (Carninci et al., 2005; Djebali et al., 2012). There is mounting evidence that lncRNAs establish specific epigenetic landscapes by guiding chromatin modifiers to distinct genomic sites (Wang and Chang, 2011). A large number of lncRNAs have been shown to repress transcription by interaction with chromatin modifiers that impair preinitiation complex formation, change nucleosome positions, or alter the epigenetic signature of specific loci (Faghihi and Wahlestedt, 2009; Guttman et al., 2011). Accordingly, lncRNAs represent an integral component of heterochromatin and are essential for the establishment and maintenance of heterochromatic features (Deng et al., 2009; Maison et al., 2011). At pericentric and telomeric regions, heterochromatin formation requires heterochromatin protein 1 (HP1) and the histone methyltransferases Suv39h and Suv4-20h. Suv39h catalyzes trimethylation of H3K9 (H3K9me3), which facilitates binding of HP1 proteins that interact with Suv4-20h and establish H4K20me3 (Schotta et al., 2004; García-Cao et al., 2004; Benetti et al., 2007). It is unknown whether HP1-dependent recruitment of Suv4-20h is restricted to pericentric and telomeric heterochromatin or whether alternative pathways exist that target Suv4-20h to chromatin.

Here we describe a lncRNA-based mechanism that guides Suv4-20h2 to rRNA genes (rDNA) to establish a more compact chromatin structure in growth-arrested cells. Previous results have established that formation of constitutive heterochromatin at murine rDNA requires pRNA, a promoter-associated RNA that recruits the chromatin remodeling complex NoRC to rDNA, triggering changes in nucleosome positioning, heterochromatic histone modifications, and DNA methylation (Li et al., 2006; Mayer et al., 2006). In addition, a fraction of rDNA is transcribed in antisense orientation by RNA polymerase II (Bierhoff et al., 2010). These antisense transcripts, termed PAPAS (*p*romoter *a*nd *p*re-rRNA *a*ntisense), comprise a heterogeneous population of lncRNA that covers the pre-rRNA coding region and the rDNA promoter. Here we show that PAPAS is upregulated in quiescent cells, elevated levels of PAPAS being accompanied by increased trimethylation of H4K20 and chromatin compaction. Gain- and loss-of-function experiments and RNA-protein binding assays revealed that PAPAS guides Suv4-20h2 to nucleolar chromatin, reinforcing quiescence-dependent transcriptional repression by mediating H4K20me3-dependent chromatin compaction. Expanding this notion, we show that intracisternal A particle (IAP) retroelements respond to growth factor deprivation by upregulating IAP-derived lncRNAs and increased levels of H4K20me3. The results uncover a novel function of lncRNA, guiding Suv4-20h2 to specific repetitive genomic loci in a manner that differs from heterochromatin formation at major satellite and telomeric repeats.

RESULTS AND DISCUSSION

Antisense Transcripts and H4K20me3 Are Upregulated at rDNA in Quiescent Cells

Repression of pre-rRNA synthesis in density-arrested or serum-deprived NIH 3T3 cells correlates with release of RNA polymerase I (Pol I) and the transcription initiation factor TIF-IA from the rDNA promoter (Figure 1A, and see Figures S1A and S1B available online). Growth arrest did not affect association of the transcription factors UBF and TIF-IB, CpG methylation, or the level of pRNA (Mayer et al., 2006), a lncRNA that triggers DNA methylation and NoRC-dependent silencing of rRNA genes (Figure S1B). However, the level of PAPAS (*p*romoter *a*nd *p*re-rRNA *a*ntisense), an antisense RNA that covers both the rDNA

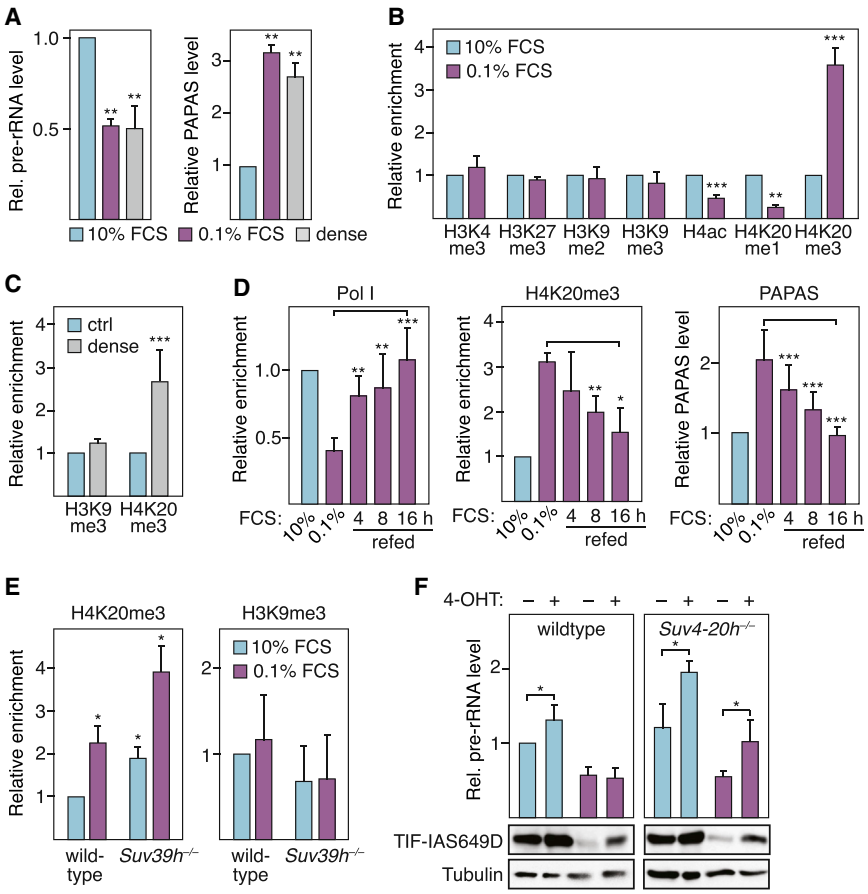

Figure 1. Inhibition of Pre-rRNA Synthesis in Quiescent Cells Correlates with Elevated Levels of PAPAS and H4K20me3

(A) RT-qPCR showing levels of pre-rRNA and PAPAS in growing (10% FCS), serum-starved (0.1% FCS), and density-arrested (dense) NIH 3T3 fibroblasts. Data were normalized to 18S rRNA.

(B) ChIP of modified histones at the rDNA promoter in NIH 3T3 cells cultured in the presence of 10% or 0.1% FCS. Data were normalized to rDNA promoter occupancy of histone H3 and are displayed as fold change upon starvation. See Figure S1C for unnormalized data.

(C) ChIP monitoring H3K9me3 and H4K20me3 in growing (ctrl) and density-arrested (dense) cells.

(D) Serum-starved cells were refed with 10% FCS for the indicated times. rDNA promoter occupancy of Pol I and H4K20me3 was assayed by ChIP; PAPAS was monitored by RT-qPCR.

(E) ChIP of H4K20me3 and H3K9me3 at rDNA in wild-type and *Suv39h*$^{-/-}$ MEFs cultured in 10% or 0.1% FCS. Data were normalized to histone H3.

(F) Levels of pre-rRNA in wild-type and *Suv4-20h*$^{-/-}$ MEFs expressing ER-tagged TIF-IAS649D. Cells were cultured in 10% or 0.1% FCS in the absence or presence of 500 nM 4-hydroxytamoxifen (4-OHT). The western blots show similar ER-TIF-IAS649D expression in wild-type and mutant MEFs.

Data are represented as SD from at least three independent replicates; *$p < 0.05$, **$p < 0.01$, ***$p < 0.001$. See also Figure S1.

promoter and the pre-rRNA coding region (Bierhoff et al., 2010) was increased (Figures 1A and S1A). The inverse correlation between the levels of PAPAS and pre-rRNA suggested that PAPAS acts in concert with signaling pathways that downregulate Pol I transcription upon growth arrest.

To assay whether changes in rDNA transcription and PAPAS levels are associated with changes in chromatin structure, we compared histone modifications at the rDNA promoter in growing and quiescent cells. Growth arrest did not affect occupancy of H3K4me3, H3K9me2, H3K9me3, and H3K27me3 but led to decreased levels of acetylated histone H4 and H4K20me1 and a 3- to 4-fold increase of H4K20me3 (Figures 1B, 1C, and S1C). PAPAS and H4K20me3 levels were also increased after cell-cycle arrest of MCF7 cells by the estrogen receptor antagonist ICI 182,780 and upon terminal differentiation of human colon cancer cells (Caco-2), C2C12 myoblasts, and 3T3-L1 cells (Figures S1D–S1G). Moreover, refeeding of starved cells with serum led to progressive binding of Pol I to rDNA, while both PAPAS and H4K20me3 decreased (Figure 1D). These results show that trimethylation of H4K20 is reversible, being enhanced upon growth arrest and decreased upon mitogenic stimulation.

Trimethylation of H4K20 at pericentric and telomeric heterochromatin depends on trimethylation of H3K9 by Suv39h (Schotta et al., 2004; García-Cao et al., 2004; Benetti et al., 2007). To examine whether the same pathway mediates quiescence-induced H4K20me3 at rDNA, we compared rDNA occupancy of H4K20me3 in wild-type and Suv39h-deficient (*Suv39h*$^{-/-}$) mouse embryonic fibroblasts (MEFs). In both cell lines H4K20me3 levels were increased upon serum deprivation (Figure 1E), indicating that gain of H4K20me3 at rDNA is independent of Suv39h activity. Knockout of ESET/Setdb1 or inhibition of G9a by BIX-01294 (Kubicek et al., 2007) did not affect upregulation of H4K20me3 (Figure S1H), demonstrating that quiescence-induced trimethylation of H4K20 does not depend on ESET/Setdb1- or G9a-mediated H3K9 methylation.

rDNA transcription requires RSK-dependent phosphorylation of TIF-IA at serine 649, which is absent in quiescent cells (Zhao et al., 2003). To examine whether both inactivation of TIF-IA and upregulation of H4K20me3 cause transcriptional repression, we monitored pre-rRNA synthesis in wild-type MEFs or *Suv4-20h*$^{-/-}$ MEFs lacking H4K20me3 (Figure S1I) after overexpression of ER-tagged TIF-IAS649D, a mutant mimicking RSK-dependent phosphorylation. Induction of ER-TIF-IAS649D with 4-hydroxytamoxifen (4-OHT) augmented pre-rRNA synthesis in both wild-type and *Suv4-20h*$^{-/-}$ MEFs. Notably, in serum-deprived *Suv4-20h*$^{-/-}$ MEFs induction of ER-TIF-IAS649D led to reactivation of pre-rRNA synthesis, whereas transcription remained repressed in wild-type MEFs (Figure 1F). This demonstrates that both mechanisms, i.e., inactivation of transcription factors and upregulation of H4K20me3, are used to throttle rRNA synthesis in resting cells. These results are in accord

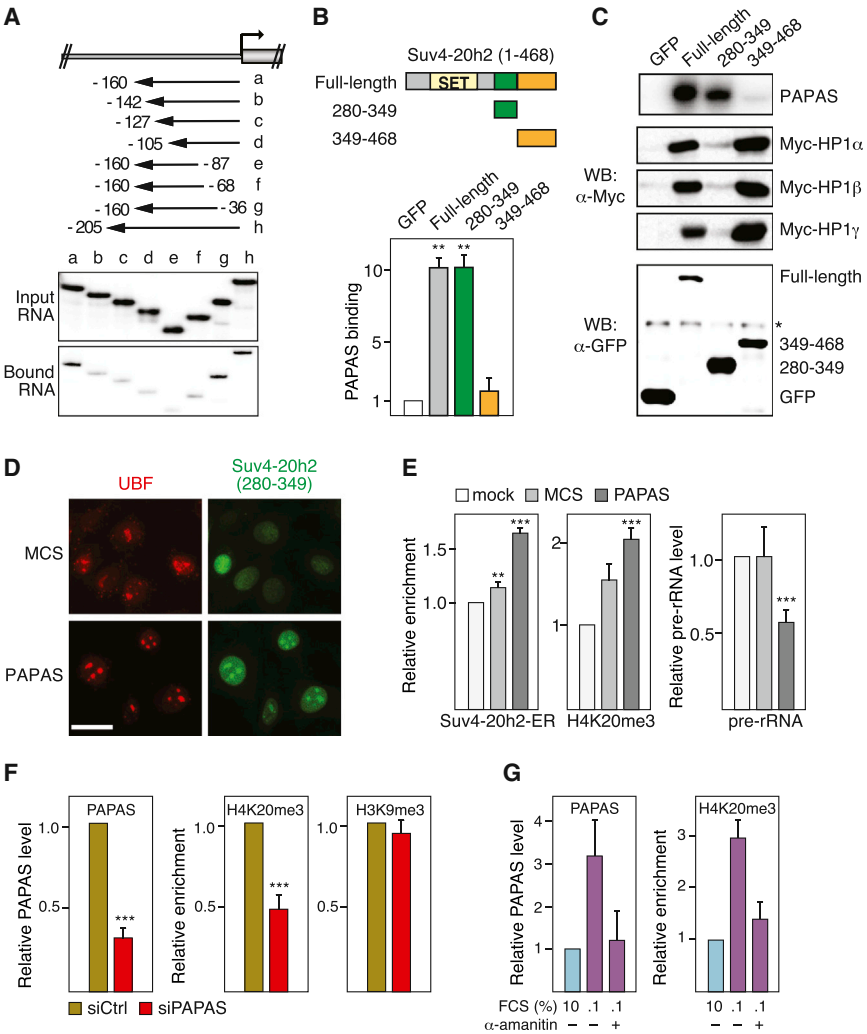

Figure 2. PAPAS Mediates H4K20me3 by Recruiting Suv4-20h2 to rDNA

(A) Pull-down assay using immobilized Suv4-20h2 and radiolabeled PAPAS truncations displayed in the scheme above. Autoradiograms of bound transcripts and 5% of input RNA are shown.

(B) RIP of GFP-tagged full-length and truncated versions of Suv4-20h2. PAPAS associated with Suv4-20h2 was assayed by RT-qPCR. Values are normalized to 18S rRNA and displayed as fold change relative to the GFP control.

(C) Different domains of Suv4-20h2 interact with PAPAS and HP1. Association of radiolabeled PAPAS (top panel) or coimmunoprecipitation of Myc-tagged HP1 isoforms (lower panels) with GFP-tagged Suv4-20h2 proteins is shown. The asterisk denotes an unspecific band in the western blot (WB).

(D) NIH 3T3 cells were transfected with control RNA (MCS) or PAPAS (−160/−1) fused to boxC/D sequences of U16 snoRNA. The immunostaining shows GFP-tagged Suv4-20h2 (280–349) and the nucleolar marker protein UBF. Scale bar, 5 μm. See Figure S2J for quantification.

(E) Ectopic PAPAS directs H4K20me3 to rDNA. Cells were transfected as in (D), and rDNA occupancy of Suv4-20h2-ER and H4K20me3 was assayed by ChIP. Pre-rRNA levels were detected by RT-qPCR. Data are presented relative to mock transfection.

(F) Knockdown of PAPAS decreases H4K20me3. Cells were transfected with control siRNA (siCtrl) or PAPAS siRNAs (siPAPAS). PAPAS was measured by RT-qPCR and rDNA occupancy of H4K20me3 and H3K9me3 by ChIP. Values represent fold change relative to siCtrl transfection.

(G) Upregulation of PAPAS and H4K20me3 depends on Pol II transcription. NIH 3T3 cells grown in 0.1% FCS were cultured in the absence or presence of α-amanitin (10 μg/ml, 12 hr). PAPAS and H4K20me3 levels were assessed by RT-qPCR and ChIP. Data were normalized to nonstarved cells (10% FCS).

In (B) and (E)–(G), data represent means ± SD from at least three independent replicates; $^{**}p < 0.01$, $^{***}p < 0.001$. See also Figure S2.

with previous studies showing that PAPAS is downregulated in a skin carcinogenesis model (Bierhoff et al., 2010), suggesting that PAPAS may safeguard postmitotic cells against the oncogenic potential of dysregulated Pol I activity (Bywater et al., 2013).

PAPAS-Directed Recruitment of Suv4-20h2 Represses rDNA Transcription

The observation that increased levels of PAPAS and H4K20me3 correlate with repression of pre-rRNA synthesis in quiescent cells suggested that PAPAS acts on active rDNA repeats, i.e., genes that are bound by UBF. In support of this view, sequential chromatin immunoprecipitation (ChIP) experiments revealed that co-occupancy of H4K20me3 with UBF increased after serum starvation (Figure S2A). The association of PAPAS with UBF-bound chromatin was also elevated in growth-arrested cells (Figures S2B and S2C), reinforcing that PAPAS and H4K20me3 are functionally linked to downregulate transcription-permissive rRNA genes.

RNA-protein interaction assays revealed preferential binding of Suv4-20h2 to PAPAS as compared to its sense counterpart (pRNA), TERRA (telomeric repeat-containing RNA) or transcripts from the multiple cloning site (MCS) of pBluescript (Figures S2D–S2F), supporting that PAPAS serves as an address label that targets Suv4-20h2 to rDNA. Interaction assays using truncated versions of PAPAS confined the binding sequence to a region comprising nucleotides −36 to −160, whereas further shortening prevented binding of PAPAS to Suv4-20h2 (Figure 2A). The minimal free energy (MFE) structure of PAPAS (−36/−160) predicts a tripartite conformation that depends on base pairing between a GAG trinucleotide (−52/−54) at the 5′ end and a CUC trinucleotide (−147/−149) at the 3′ end (Figure S2G). Mutation of the GAG trinucleotide impaired the interaction with Suv4-20h2, while a compensatory mutation of the CUC trinucleotide

restored binding, emphasizing the relevance of the GAG/CUC base pairing for Suv4-20h2 binding to PAPAS.

To demonstrate association of Suv4-20h2 with PAPAS in vivo, we monitored binding of PAPAS by RNA immunoprecipitation (RIP) experiments, using full-length Suv4-20h2 and two truncation mutants comprising either the internal part of Suv4-20h2 (aa 280–349), predicted to exhibit RNA binding activity (Figure S2H), or the C-terminal part (aa 349–468) that interacts with HP1 and is required for association with pericentric heterochromatin (Schotta et al., 2004; Hahn et al., 2013). Suv4-20h2 comprising aa 280–349 bound to PAPAS like full-length Suv4-20h2, whereas the C-terminal part did not interact (Figure 2B). Pull-down and coimmunoprecipitation experiments confirmed that the internal part of Suv4-20h2 mediates the interaction with RNA, whereas the C-terminal part interacts with HP1 (Figure 2C). In accord with PAPAS targeting Suv4-20h2 to transcription-competent rDNA repeats, both full-length Suv4-20h2 and the internal part were enriched at rDNA in serum-starved cells (Figure S2I). Assay of CpG-methylation of Suv4-20h2-associated rDNA by methylation-specific restriction analysis (Santoro et al., 2002) revealed that the internal part of Suv4-20h2 was preferentially associated with active, unmethylated rRNA genes, while the C-terminal part of Suv4-20h2 was bound to methylated, silent rDNA promoters (Figure S2I). Occupancy of Suv4-20h2 and H4K20me3 was partly shifted from methylated to unmethylated genes in response to serum starvation, reinforcing that HP1 tethers Suv4-20h2 to silent rDNA repeats, whereas quiescence-induced PAPAS recruits Suv4-20h2 to transcription-competent rRNA genes.

To examine whether ectopic PAPAS is capable to recruit Suv4-20h2 to rDNA, we transfected cells with PAPAS-boxC/D, a fusion of PAPAS sequences (from −1 to −160) that interact with Suv4-20h2 with boxC/D sequences of U16 snoRNA that direct nucleolar localization (Lange et al., 1998; Michienzi et al., 2000). In support of PAPAS targeting Suv4-20h2 to rDNA, ectopic PAPAS caused nucleolar enrichment of the internal part of Suv4-20h2, whereas transfection of control RNA (MCS-RNA-boxC/D) did not affect Suv4-20h2 localization (Figures 2D, S2J, and S2K). Transfection of PAPAS-boxC/D also led to increased rDNA occupancy of Suv4-20h2-ER and H4K20me3 as well as repression of pre-rRNA synthesis (Figure 2E). Conversely, knockdown of endogenous PAPAS with siRNA or LNA/DNA oligonucleotides decreased H4K20me3, but not H3K9me3 (Figures 2F and S2L). In accord with PAPAS being transcribed by RNA polymerase II (Bierhoff et al., 2010), α-amanitin treatment prevented upregulation of PAPAS and H4K20me3 in serum-deprived cells (Figure 2G), emphasizing that increased trimethylation of H4K20 requires elevated levels of PAPAS.

H4K20me3 Facilitates Global Chromatin Compaction in Quiescent Cells

H4K20me3 has been shown to compact chromatin in vitro (Lu et al., 2008), raising the possibility that PAPAS-mediated trimethylation of H4K20 alters chromatin accessibility in quiescent cells. To decipher the link between repression of rDNA transcription, H4K20 trimethylation and chromatin structure, we monitored chromatin accessibility by FAIRE (Formaldehyde Assisted Isolation of Regulatory Elements), an assay that measures nucleosome density according to extractability of crosslinked chromatin (Simon et al., 2012). In serum-deprived NIH 3T3 cells the fraction of extractable rDNA was significantly reduced, whereas the recovery of subtelomeric repeats was not affected (Figure 3A). A more compact, less extractable chromatin structure was also observed in serum-deprived wild-type MEFs. In contrast, the extractability of rDNA was not affected in *Suv4-20h*$^{-/-}$ MEFs (Figure 3B), underscoring the essential role of Suv4-20h2-dependent H4K20 trimethylation in the establishment of a repressive chromatin state.

Increased chromatin compaction was confirmed by probing chromatin accessibility by micrococcal nuclease (MNase) digestion. In accord with a recent study showing global chromatin compaction and upregulation of H4K20me3 in contact-inhibited human fibroblasts (Evertts et al., 2013), quiescent NIH 3T3 cells and wild-type MEFs exhibited a chromatin structure that is less accessible to MNase digestion (Figures 3C, 3D, and S3A). In contrast, chromatin from *Suv4-20h*$^{-/-}$ MEFs was readily digested, regardless of whether cells were cultured in 10% or 0.1% serum, indicating that H4K20me3-mediated chromatin compaction alters global chromatin structure in response to growth arrest. In support of H4K20me3 rather than other histone modifications being causally involved in this process, there was a significant increase in the global level of H4K20me3 and a concomitant decrease of H4K20me1 in serum-deprived cells, whereas trimethylation states of H3K4, H3K9, and H3K27 were not affected (Figures 3E and S3B). After refeeding with serum, H4K20me3 levels declined to basal levels within 8 hr (Figure S3C). This demonstrates that trimethylation of H4K20 is a dynamic process, quiescence-induced H4K20me3 being reverted when cells re-enter the cell cycle. Notably, the global increase in H4K20me3 in response to serum deprivation was also observed in *Suv39h*$^{-/-}$ and *Setdb1*$^{-/-}$ MEFs and after pharmacological inhibition of the methyltransferase G9a, reinforcing that quiescence-induced changes in chromatin structure do not depend on di- or trimethylation of H3K9 (Figures 3F, S3D, and S3E). Treatment with α-amanitin, on the other hand, prevented the increase in H4K20me3 in serum-deprived cells (Figure 3G), underscoring that upregulation of H4K20me3 requires Pol II transcription.

IAP Retroelements Are Silenced by lncRNA-Mediated H4K20me3

The global increase of H4K20me3 in quiescent cells suggested that upregulation of H4K20me3 is not restricted to rRNA genes but may also occur at other abundant genomic elements. We focused on IAP retrotransposons that account for ~3% of the genome, exhibit high levels of H4K20me3 even in Suv39h-deficient cells (Martens et al., 2005), and are partially derepressed in growing and starved *Suv4-20h*$^{-/-}$ MEFs (Figure S4A). Upon serum starvation, Suv4-20h2-ER and H4K20me3, but not H3K9me3, increased 2-fold at IAP elements, while binding to subtelomeric repeats remained unchanged (Figures 4A and S4B). FAIRE assays showed that IAP chromatin was less extractable from growth-arrested cells (Figure 4B), demonstrating that H4K20me3-mediated chromatin compaction is not restricted to rRNA genes but also occurs at IAP retrotransposons.

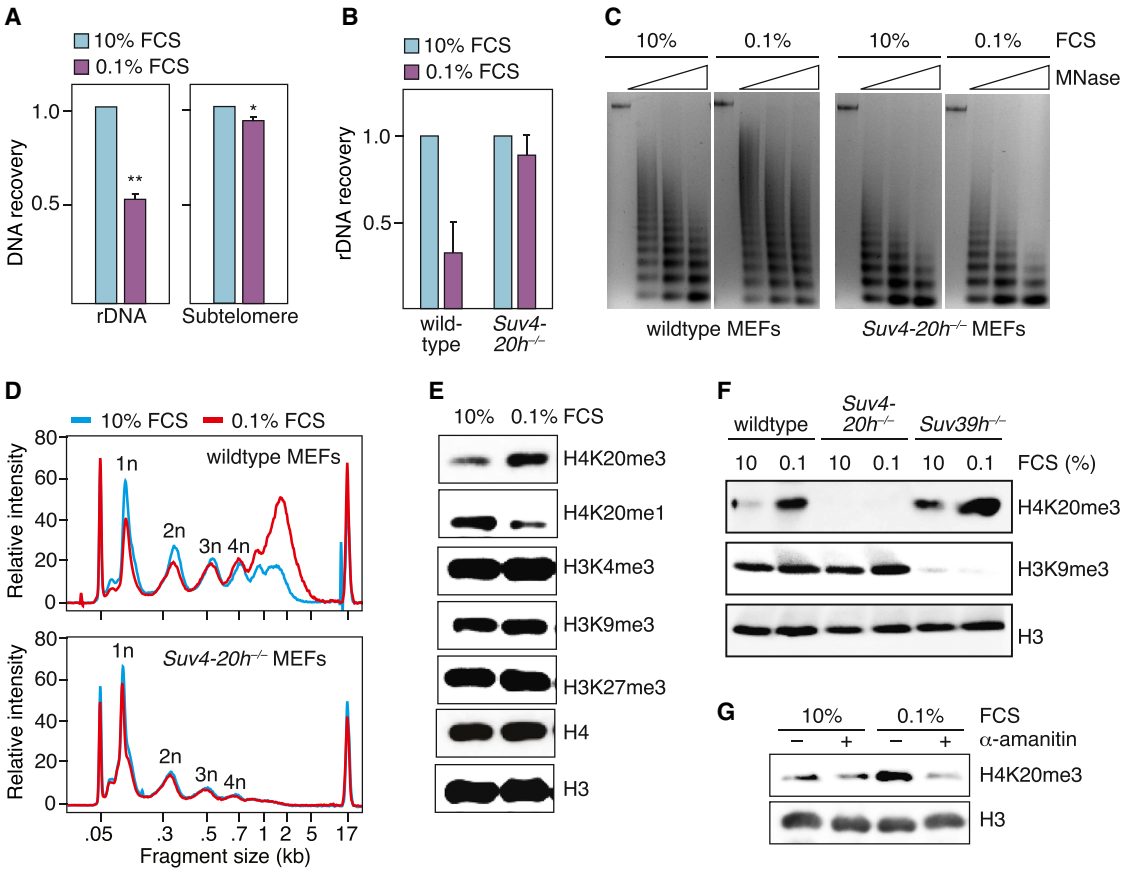

Figure 3. Upregulation of H4K20me3 in Growth-Arrested Cells Leads to Chromatin Compaction

(A) Shown is FAIRE assay monitoring chromatin extractability of NIH 3T3 cells cultured in the presence of 10% or 0.1% FCS. Recovered DNA was quantified by qPCR using primers for rDNA (−160/–1) or subtelomeres of chromosome 19. Data represent means ± SD; *$p < 0.05$, **$p < 0.01$.

(B) FAIRE assay in wild-type and *Suv4-20h*$^{-/-}$ MEFs. rDNA (−160/−1) was assayed by qPCR and normalized to an intergenic spacer sequence (+19,614/+19,761). Error bars indicate SD.

(C) Global chromatin compaction upon growth arrest. Nuclei from MEFs cultured in 10% or 0.1% FCS were digested with 0, 0.5, 1, and 2 U of micrococcal nuclease (MNase) and DNA was analyzed by gel electrophoresis.

(D) Chromatin from wild-type and *Suv4-20h*$^{-/-}$ MEFs digested with 2 U MNase was monitored on a Bioanalyzer. Nucleosomal fragments are indicated (1n–4n).

(E) Western blots showing global upregulation of H4K20me3 in serum-deprived cells. Histones were extracted from NIH 3T3 cells cultured in 10% or 0.1% FCS, and the indicated modifications were monitored on immunoblots.

(F) Western blots monitoring H4K20me3 and H3K9me3 levels in growing and serum-starved wild-type and mutant MEFs.

(G) Upregulation of H4K20me3 requires Pol II transcription. NIH 3T3 cells in 10% or 0.1% FCS were treated with α-amanitin (10 μg/ml, 12 hr), and H4K20me3 was monitored on immunoblots.

See also Figure S3.

Given that retrotransposition is abolished in nonproliferating cells (Kubo et al., 2006; Shi et al., 2007), we reasoned that epigenetic changes at IAP elements are causally involved in quiescence-induced transcriptional silencing and inhibition of retrotransposition. In accord with transcription of IAPs being repressed in growth-arrested cells, a 50% decrease in the amount of IAP-specific ~7 kb full-length transcripts was detected on northern blots (Figures 4C). On the other hand, low abundant 15–20 kb long RNAs were ~2-fold increased. These IAP-specific lncRNAs are associated with chromatin and originate upstream of the 5′ long terminal repeats (LTRs) (Figures 4D and S4C). The intriguing correlation between the global increase in H4K20me3 and elevated levels of IAP-specific lncRNA suggested that recruitment of Suv4-20h2 to IAP elements occurs in a similar way as PAPAS-dependent targeting to rDNA. To examine whether Suv4-20h2 interacts with IAP-specifc RNA, we performed binding assays using a *Gag* transcript that is contained in the short and long IAP RNA. These experiments revealed that the internal part of Suv4-20h2 binds to IAP transcripts in vivo and in vitro (Figures 4E and S4D). Other Suv4-20h2 binding sites reside in the lncRNA-specific 5′ and 3′ LTR regions, suggesting that the 15–20 kb IAP RNA can target Suv4-20h2 by multiple interactions (Figure S4E). Knockdown of IAP lncRNA with LNA/DNA gapmers encompassing LTR sequences led to upregulation of the major 7 kb transcript, supporting that the IAP lncRNA mediates recruitment of Suv4-20h2 and repression of IAP transcription (Figure S4F).

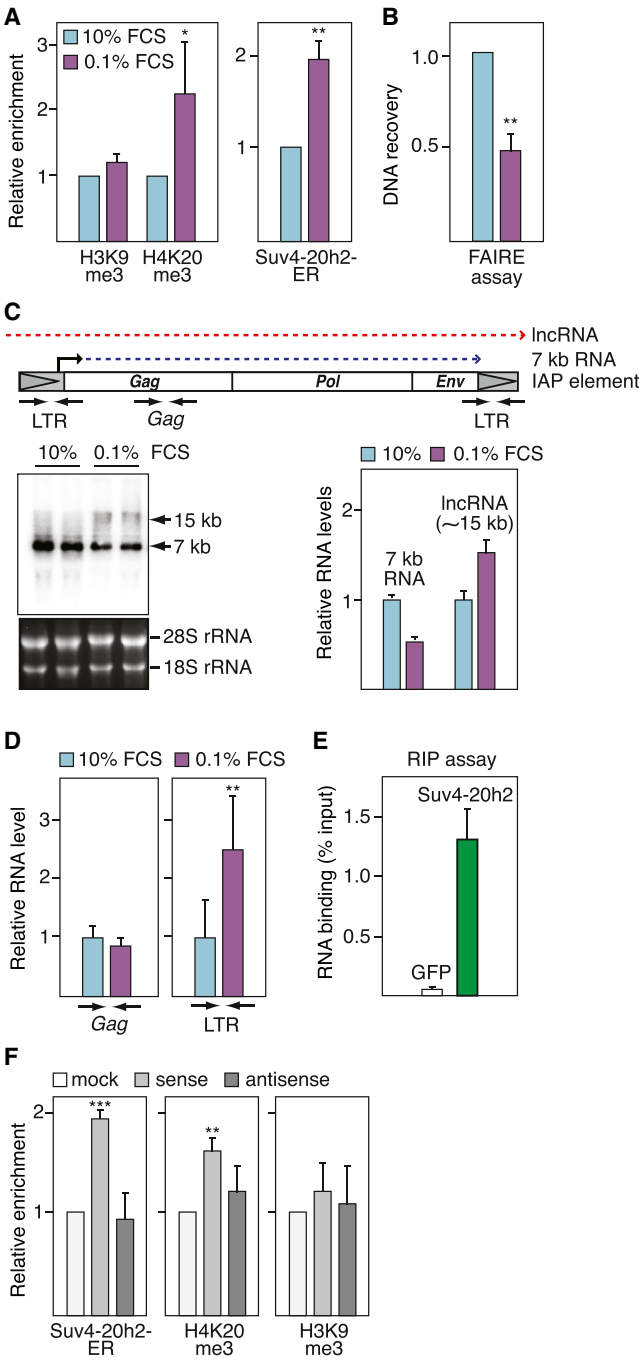

Figure 4. Interaction of IAP-Specific lncRNA with Suv4-20h2 Triggers H4K20me3

(A) ChIP of H3K9me3, H4K20me3, and Suv4-20h2-ER at IAP retroelements in growing (10% FCS) or starved (0.1% FCS) NIH 3T3 cells. Levels of histone modifications were normalized to histone H3. Binding of Suv4-20h2-ER was normalized to subtelomeres of chromosome 19.

(B) FAIRE assay measuring chromatin compaction at IAP elements. Extraction of IAP DNA from growing and starved cells was quantified by qPCR using primers amplifying the *Gag* region.

(C) Northern blot of IAP-specific transcripts. NIH 3T3 cells were cultured in 10% or 0.1% FCS, and IAP RNA was detected with a *Gag* riboprobe. EtBr-stained rRNA is shown below. The ~7 kb major transcripts and ~15 kb lncRNAs are indicated in the scheme above. The bar diagram depicts quantification of IAP RNAs relative to 28S rRNA.

(D) RT-qPCR showing quiescence-induced IAP-specific lncRNAs. cDNA was synthesized with the *Gag* reverse primer followed by qPCR with *Gag* primers to measure total IAP RNA (left) or with LTR primers to identify IAP lncRNA (right).

(E) RIP showing association of IAP transcripts with GFP-tagged Suv4-20h2. Coprecipitated IAP RNA was assayed by RT-qPCR and normalized to input RNA.

(F) IAP-specific RNA recruits Suv4-20h2. NIH 3T3 cells were transfected with 500 ng of sense or antisense *Gag* transcripts, and occupancy of Suv4-20h2-ER, H4K20me3, and H3K9me3 at IAP elements was assessed by ChIP. Data are shown as fold change relative to transfections without RNA.

Data are represented as mean ± SD from at least three independent replicates; *p < 0.05, **p < 0.01, ***p < 0.001. See also Figure S4.

If lncRNA guides Suv4-20h2 to IAP elements, ectopic IAP-specific RNA should elevate H4K20me3. Indeed, transfection of RNA comprising IAP sequences that interact with Suv4-20h2 led to enhanced occupancy of both Suv4-20h2-ER and H4K20me3 at IAPs, while H3K9me3 levels did not change (Figure 4F). Synthetic transcripts in antisense orientation had no effect on Suv4-20h2 and H4K20me3 binding, reinforcing that IAP-specific sense transcripts facilitate recruitment of Suv4-20h2. Together, these results indicate that similar mechanisms mediate changes in chromatin states at rDNA and IAP elements in quiescent cells, depending on upregulation of lncRNAs that recruit Suv4-20h2 to trigger H4K20 trimethylation and chromatin compaction.

The results of this study demonstrate that trimethylation of H4K20 is important to establish a specific chromatin structure at distinct repetitive sequences upon growth arrest. At rDNA clusters, H4K20me3-induced chromatin compaction throttles pre-rRNA synthesis after growth factor deprivation and upon terminal differentiation, reinforcing cell-cycle exit. At IAP elements, chromatin compaction likely impairs retrotransposition in postmitotic cells that cannot employ high-fidelity homologous recombination between sister chromatids. Therefore, high levels of H4K20me3 in somatic cells are important to counteract cancer-associated somatic transposition (Lee et al., 2012), providing a molecular explanation for why H4K20me3 is progressively lost in human tumors (Fraga et al., 2005). An emerging theme among lncRNA functions is the regulation of cell fate decisions in somatic tissue, often in response to environmental cues (Hu et al., 2011; Kretz et al., 2012, 2013). Further elucidation of how PAPAS and other Suv4-20h2-interacting lncRNAs are regulated in response to growth-factor availability and differentiation signals will provide insights into how chromatin structure and gene expression are balanced between proliferation and quiescence.

EXPERIMENTAL PROCEDURES

Cell Culture, Transfection, and Retroviral Infection

Cells were cultured at 37°C and 5% CO_2 with 10% fetal calf serum (FCS). Serum-starved cells were maintained for 36–48 hr in 0.1% FCS. Plasmids were transfected by calcium phosphate coprecipitation, and RNA and LNA/DNA oligonucleotides were transfected with *Trans*IT TKO reagent (Mirus) and siRNAs with Lipofectamine RNAiMAX (Life Technologies). For retroviral infections, pBabe-puro viruses were produced in ecotropic Phoenix cells. Plasmids and cell differentiation methods are detailed in Supplemental Information.

RNA Analysis and In Vitro Transcription

Cellular RNA was isolated with Tri-Reagent (Sigma) and reverse transcribed using M-MLV (Life Technologies) and either random hexamers or sequence-specific primers (see Table S1). PAPAS cDNA was synthesized with RT-primers fused to the T7 promoter sequence, and cDNA was PCR-amplified with T7 forward primer and rDNA-specific reverse primer. Synthetic RNAs were generated by in vitro transcription and purified using the RNeasy Mini kit (QIAGEN). Details are provided in the Supplemental Information.

Pull-Down Assays and RNA Immunoprecipitation

For RNA pull-down, GFP-tagged Suv4-20h2 was expressed in HEK293T cells, immobilized on GFP-Trap agarose (ChromoTek), and incubated with radiolabeled transcripts for 1 hr at room temperature. Captured RNA was eluted with formamide, run on 6% denaturating polyacrylamide gels, and visualized by PhosphorImaging. Suv4-20h2-GFP was pulled down from HEK293T cell lysates with biotinylated transcripts immobilized on streptavidin-coupled Dynabeads (Invitrogen) followed by western blotting. For RIP, Suv4-20h2-GFP was precipitated from NIH 3T3 cells with GFP-Trap, and bound RNA was analyzed by RT-qPCR. For details, see Supplemental Information.

Chromatin Immunoprecipitation

ChIP and ChRIP assays were performed as detailed in the Supplemental Information. Precipitated DNA was subjected to qPCR and normalized to input DNA. ChIPs of modified histones were normalized to unmodified histone H3. Primers are listed in Table S1.

Chromatin Accessibility Assays

FAIRE assays were performed according to Simon et al. (2012) followed by qPCR. To analyze global chromatin compaction, nuclei were digested with micrococcal nuclease (MNase, Sigma), and nucleosomal DNA was analyzed on agarose gels or with an Agilent 2100 bioanalyzer (Agilent Technologies). Details for chromatin accessibility assays are provided in the Supplemental Information.

Statistical Analysis

Data are reported as mean values from at least three biological replicates with error bars denoting standard deviations (SD). Comparison between two groups were performed using a paired two-tailed Student's t test, p values $^{*}p < 0.05$, $^{**}p < 0.01$, and $^{***}p < 0.001$.

SUPPLEMENTAL INFORMATION

Supplemental Information includes four figures, one table, and Supplemental Experimental Procedures and can be found with this article at http://dx.doi.org/10.1016/j.molcel.2014.03.032.

ACKNOWLEDGMENTS

We thank T. Jenuwein and R. Fan for providing *Suv39h*$^{-/-}$ and *Setdb1*$^{-/-}$ MEFs, M. Hahn for Suv4-20h2 expression plasmids, and C. Maul and B. Dörr for technical assistance. This work has been supported by the DFG (GR475/22-1 and SFB 1064), the BMBF (0315502A "EpiSys"), and the ERC (232645).

Received: November 6, 2013
Revised: January 31, 2014
Accepted: March 10, 2014
Published: April 24, 2014

REFERENCES

Benetti, R., Gonzalo, S., Jaco, I., Schotta, G., Klatt, P., Jenuwein, T., and Blasco, M.A. (2007). Suv4-20h deficiency results in telomere elongation and derepression of telomere recombination. J. Cell Biol. *178*, 925–936.

Bierhoff, H., Schmitz, K., Maass, F., Ye, J., and Grummt, I. (2010). Noncoding transcripts in sense and antisense orientation regulate the epigenetic state of ribosomal RNA genes. Cold Spring Harb. Symp. Quant. Biol. *75*, 357–364.

Bywater, M.J., Pearson, R.B., McArthur, G.A., and Hannan, R.D. (2013). Dysregulation of the basal RNA polymerase transcription apparatus in cancer. Nat. Rev. Cancer *13*, 299–314.

Carninci, P., Kasukawa, T., Katayama, S., Gough, J., Frith, M.C., Maeda, N., Oyama, R., Ravasi, T., Lenhard, B., Wells, C., et al.; FANTOM Consortium; RIKEN Genome Exploration Research Group and Genome Science Group (Genome Network Project Core Group) (2005). The transcriptional landscape of the mammalian genome. Science *309*, 1559–1563.

Deng, Z., Norseen, J., Wiedmer, A., Riethman, H., and Lieberman, P.M. (2009). TERRA RNA binding to TRF2 facilitates heterochromatin formation and ORC recruitment at telomeres. Mol. Cell *35*, 403–413.

Djebali, S., Davis, C.A., Merkel, A., Dobin, A., Lassmann, T., Mortazavi, A., Tanzer, A., Lagarde, J., Lin, W., Schlesinger, F., et al. (2012). Landscape of transcription in human cells. Nature *489*, 101–108.

Evertts, A.G., Manning, A.L., Wang, X., Dyson, N.J., Garcia, B.A., and Coller, H.A. (2013). H4K20 methylation regulates quiescence and chromatin compaction. Mol. Biol. Cell *24*, 3025–3037.

Faghihi, M.A., and Wahlestedt, C. (2009). Regulatory roles of natural antisense transcripts. Nat. Rev. Mol. Cell Biol. *10*, 637–643.

Fraga, M.F., Ballestar, E., Villar-Garea, A., Boix-Chornet, M., Espada, J., Schotta, G., Bonaldi, T., Haydon, C., Ropero, S., Petrie, K., et al. (2005). Loss of acetylation at Lys16 and trimethylation at Lys20 of histone H4 is a common hallmark of human cancer. Nat. Genet. *37*, 391–400.

García-Cao, M., O'Sullivan, R., Peters, A.H., Jenuwein, T., and Blasco, M.A. (2004). Epigenetic regulation of telomere length in mammalian cells by the Suv39h1 and Suv39h2 histone methyltransferases. Nat. Genet. *36*, 94–99.

Guttman, M., Donaghey, J., Carey, B.W., Garber, M., Grenier, J.K., Munson, G., Young, G., Lucas, A.B., Ach, R., Bruhn, L., et al. (2011). lincRNAs act in the circuitry controlling pluripotency and differentiation. Nature *477*, 295–300.

Hahn, M., Dambacher, S., Dulev, S., Kuznetsova, A.Y., Eck, S., Wörz, S., Sadic, D., Schulte, M., Mallm, J.P., Maiser, A., et al. (2013). Suv4-20h2 mediates chromatin compaction and is important for cohesin recruitment to heterochromatin. Genes Dev. *27*, 859–872.

Hu, W., Yuan, B., Flygare, J., and Lodish, H.F. (2011). Long noncoding RNA-mediated anti-apoptotic activity in murine erythroid terminal differentiation. Genes Dev. *25*, 2573–2578.

Kretz, M., Webster, D.E., Flockhart, R.J., Lee, C.S., Zehnder, A., Lopez-Pajares, V., Qu, K., Zheng, G.X., Chow, J., Kim, G.E., et al. (2012). Suppression of progenitor differentiation requires the long noncoding RNA ANCR. Genes Dev. *26*, 338–343.

Kretz, M., Siprashvili, Z., Chu, C., Webster, D.E., Zehnder, A., Qu, K., Lee, C.S., Flockhart, R.J., Groff, A.F., Chow, J., et al. (2013). Control of somatic tissue differentiation by the long non-coding RNA TINCR. Nature *493*, 231–235.

Kubicek, S., O'Sullivan, R.J., August, E.M., Hickey, E.R., Zhang, Q., Teodoro, M.L., Rea, S., Mechtler, K., Kowalski, J.A., Homon, C.A., et al. (2007). Reversal of H3K9me2 by a small-molecule inhibitor for the G9a histone methyltransferase. Mol. Cell *25*, 473–481.

Kubo, S., Seleme, M.C., Soifer, H.S., Perez, J.L., Moran, J.V., Kazazian, H.H., Jr., and Kasahara, N. (2006). L1 retrotransposition in nondividing and primary human somatic cells. Proc. Natl. Acad. Sci. USA *103*, 8036–8041.

Lange, T.S., Borovjagin, A., Maxwell, E.S., and Gerbi, S.A. (1998). Conserved boxes C and D are essential nucleolar localization elements of U14 and U8 snoRNAs. EMBO J. *17*, 3176–3187.

Lee, E., Iskow, R., Yang, L., Gokcumen, O., Haseley, P., Luquette, L.J., 3rd, Lohr, J.G., Harris, C.C., Ding, L., Wilson, R.K., et al.; Cancer Genome Atlas Research Network (2012). Landscape of somatic retrotransposition in human cancers. Science *337*, 967–971.

Li, J., Längst, G., and Grummt, I. (2006). NoRC-dependent nucleosome positioning silences rRNA genes. EMBO J. *25*, 5735–5741.

Lu, X., Simon, M.D., Chodaparambil, J.V., Hansen, J.C., Shokat, K.M., and Luger, K. (2008). The effect of H3K79 dimethylation and H4K20 trimethylation on nucleosome and chromatin structure. Nat. Struct. Mol. Biol. *15*, 1122–1124.

Maison, C., Bailly, D., Roche, D., Montes de Oca, R., Probst, A.V., Vassias, I., Dingli, F., Lombard, B., Loew, D., Quivy, J.P., and Almouzni, G. (2011). SUMOylation promotes de novo targeting of HP1α to pericentric heterochromatin. Nat. Genet. *43*, 220–227.

Martens, J.H., O'Sullivan, R.J., Braunschweig, U., Opravil, S., Radolf, M., Steinlein, P., and Jenuwein, T. (2005). The profile of repeat-associated histone lysine methylation states in the mouse epigenome. EMBO J. *24*, 800–812.

Mayer, C., Schmitz, K.M., Li, J., Grummt, I., and Santoro, R. (2006). Intergenic transcripts regulate the epigenetic state of rRNA genes. Mol. Cell *22*, 351–361.

Michienzi, A., Cagnon, L., Bahner, I., and Rossi, J.J. (2000). Ribozyme-mediated inhibition of HIV 1 suggests nucleolar trafficking of HIV-1 RNA. Proc. Natl. Acad. Sci. USA *97*, 8955–8960.

Santoro, R., Li, J., and Grummt, I. (2002). The nucleolar remodeling complex NoRC mediates heterochromatin formation and silencing of ribosomal gene transcription. Nat. Genet. *32*, 393–396.

Schotta, G., Lachner, M., Sarma, K., Ebert, A., Sengupta, R., Reuter, G., Reinberg, D., and Jenuwein, T. (2004). A silencing pathway to induce H3-K9 and H4-K20 trimethylation at constitutive heterochromatin. Genes Dev. *18*, 1251–1262.

Shi, X., Seluanov, A., and Gorbunova, V. (2007). Cell divisions are required for L1 retrotransposition. Mol. Cell. Biol. *27*, 1264–1270.

Simon, J.M., Giresi, P.G., Davis, I.J., and Lieb, J.D. (2012). Using formaldehyde-assisted isolation of regulatory elements (FAIRE) to isolate active regulatory DNA. Nat. Protoc. *7*, 256–267.

Wang, K.C., and Chang, H.Y. (2011). Molecular mechanisms of long noncoding RNAs. Mol. Cell *43*, 904–914.

Zhao, J., Yuan, X., Frödin, M., and Grummt, I. (2003). ERK-dependent phosphorylation of the transcription initiation factor TIF-IA is required for RNA polymerase I transcription and cell growth. Mol. Cell *11*, 405–413.